IJC Heart & Vasculature 44 (2023) 101167

Contents lists available at ScienceDirect

IJC Heart & Vasculature

journal homepage: www.sciencedirect.com/journal/ijc-heart-and-vasculature

CMR-based right ventricular strain analysis in cardiac amyloidosis and its potential as a supportive diagnostic feature

Jan Eckstein [a], Hermann Körperich [a,*], Elena Weise Valdés [a], Vanessa Sciacca [b], Lech Paluszkiewicz [c], Wolfgang Burchert [a], Martin Farr [d], Philipp Sommer [b], Christian Sohns [b], Misagh Piran [a]

[a] Institute for Radiology, Nuclear Medicine and Molecular Imaging, Heart and Diabetes Center North Rhine Westphalia, Bad Oeynhausen, University of Bochum, Germany
[b] Clinic for Electrophysiology, Heart and Diabetes Center North Rhine Westphalia, Bad Oeynhausen, University of Bochum, Germany
[c] Clinic for Thoracic and Cardiovascular Surgery, Heart and Diabetes Center North-Rhine Westphalia, Ruhr-University of Bochum, Bad Oeynhausen, Germany
[d] Cardiogenetic Laboratory, Heart and Diabetes Center North-Rhine Westphalia, Ruhr-University of Bochum, Bad Oeynhausen, Germany

ARTICLE INFO

Keywords:
Cardiovascular magnetic resonance imaging
Cardiac amyloidosis
Hypertrophic phenotype
Global and regional strain
Amyloidosis subtypes

ABSTRACT

Background: Right ventricular (RV) strain has provided valuable prognostic information for patients with cardiac amyloidosis (CA). However, the extent to which RV strain and strain rate can differentiate CA is not yet clinically established. CA underdiagnosis delays treatment strategies and exacerbates patient prognosis.
Aims: Evaluation of cardiac magnetic resonance (CMR) quantified RV global and regional strain of CA and HCM patients along with CA subtypes.
Methods: CMR feature tracking attained longitudinal, radial and circumferential global and regional strain in 47 control subjects (CTRL), 43 CA-, 20 hypertrophic cardiomyopathy- (HCM) patients. CA patients were subdivided in 21 transthyretin-related amyloidosis (ATTR) and 20 acquired immunoglobulin light chain (AL) patients. Strain data and baseline clinical parameters were statistically analysed with respect to diagnostic performance and discriminatory power between the different clinical entities.
Results: Effective differentiation of CA from HCM patients was achieved utilizing global longitudinal (GLS: 16.5 ± 3.9% vs. −21.3 ± 6.7%, $p = 0.032$), radial (GRS: 11.7 ± 5.3% vs. 16.5 ± 7.1%, $p < 0.001$) and circumferential (GCS: -7.6 ± 4.0% vs. −9.4 ± 4.4%, $p = 0.015$) right ventricular strain. Highest strain-based hypertrophic phenotype differentiation was attained using GRS (AUC = 0.86). Binomial regression found right ventricular ejection fraction (RV-EF) ($p = 0.017$) to be a significant predictor of CA-HCM differentiation. CA subtypes had comparable cardiac strains.
Conclusion: CMR-derived RV global strains and various regional longitudinal strains provide discriminative radiological features for CA-HCM differentiation. However, in terms of feasibility, cine-derived RV-EF quantification may suffice for efficient differential diagnostic support.

1. Introduction

Right ventricular involvement in patients with cardiac amyloidosis (CA) is associated with worsening clinical prognosis [1]. Differentiation of the hypertrophic phenotype is complex and carries the risk of underdiagnosing CA, leading to delay of necessary therapeutic measures. Quantification of cardiac strain by echocardiography and cardiac magnetic resonance imaging (CMR) is gaining diagnostic value for the differentiation of amyloidosis, with most studies focusing on the left atrium and left ventricle [2–7]. To date, CMR studies of the right ventricle, particularly regarding strain as a diagnostic feature for disease discrimination, remain scarce and its clinical value largely unknown.

Recent echocardiographic findings of the right ventricle have shown that basal free wall systolic strain and TAPSE are accurate parameters for the early diagnosis of light chain cardiac amyloidosis (AL) in patients with otherwise normal echocardiographic features [8]. Among CA

* Corresponding author at: Herz- und Diabeteszentrum NRW, Ruhr-Universität Bochum, Institut für Radiologie, Nuklearmedizin und Molekulare Bildgebung, Georgstr. 11, 32545 Bad Oeynhausen, Germany.
E-mail address: hkoerperich@hdz-nrw.de (H. Körperich).

https://doi.org/10.1016/j.ijcha.2022.101167
Received 17 July 2022; Received in revised form 11 October 2022; Accepted 23 December 2022

patients with the transthyretin subtype (ATTR) no early echocardiographic markers were identified. However, right ventricular basal and apical longitudinal peak systolic strain differentiate significantly from hypertrophic cardiomyopathy (HCM) patients [9]. However, due to limitations in acoustic windows, operator dependence and spatial resolution, CMR has set the gold standard for comprehensive assessment of the right ventricle [10]. To the best of our knowledge, only one CMR study has addressed the discriminatory role of right ventricular strain in distinguishing between CA and HCM patients [11]. Their findings of global right ventricular strains were suggestive of CA dependent strain variations that may support differential diagnostics between CA and HCM patients. Recent studies have already demonstrated the prognostic and diagnostic value of left ventricular strain, T1 mapping and late gadolinium enhancement for improved CA detection at ventricular and atrial level [5,12–16]. Although effective strain differentiation has been presented using the left ventricle, its limitations must be noted. Per example, in a sub-analysis by Giusca et al. [5], patients with mild to moderate hypertrophy presented no significant difference in strain derived % normal myocardium between HCM and CA patients. This highlights the value of conducting multiple chamber analyses, which presumably results in greater diagnostic sensitivity and specificity. However, this study conducted a comprehensive analysis for diagnostic differences in global right ventricular longitudinal, circumferential and radial strains and right ventricular regional basal, mid and apical strains between CA and HCM patients. A comparison with healthy control subjects was provided. To date, late gadolinium enhancement (LGE) assessment of left ventricular myocardium plays a central role in the differential diagnosis of the hypertrophic phenotype. However, renal insufficiency is not uncommon in amyloidotic patients and cardiac strain may pose a valuable non-contrast diagnostic alternative. Predictive value of baseline clinical parameters was further elucidated as pure reliance on strain values may be associated with false positive diagnostics as both patient groups can be presumed to have abnormal right ventricular function and deformation. This assessment may reiterate the purpose of multi-parametric validation. Additionally, diagnostic performance of right ventricular strain and strain rate was assessed for CA subtypes ATTR and AL.

2. Methods

2.1. Study population

This is a single center case control study. CA patients were enrolled upon biopsy-validation, subtype identification and adequate CMR quality. HCM were included after confirmed diagnosis according to ESC guidelines 2014 and AHA guidelines 2020 [17,18]. A group of healthy controls (CTRL) aged over 50 years were provided. A written informed consent was obtained from all participants and patients. CTRL subjects were only included if no cardiovascular or metabolic disease, surgery, risk factors, or medication were reported according to the in-hospital questionnaire (supplement “Questionnaire”), which corresponds to the NYHA-I classification (heart disease without physical limitations, whereby daily physical strain does not cause inadequate fatigue, arrhythmias, shortness of breath or angina pectoris). Exclusion criteria for CTRL subjects entailed CMR identified myocardial abnormalities, aortic ectasia, pulmonary trunk dilation, ischemic heart disease, valvular heart disease, indications of cardiomyopathy. All examinations were conducted in accordance with the 1964 declaration of Helsinki and the study was approved by the local ethics committee (Ethik-Kommission der Medizinischen Fakultät der Ruhr-Universität Bochum; registration number 2017–238).

2.2. Cardiac MRI

All subjects underwent CMR at our institution using a 3.0 Tesla multi-transmit magnetic resonance imaging system (Achieva, Philips Healthcare, Best, The Netherlands; Release 5.3.1 and 5.6.1) incorporating dStream technology. Vector electrocardiogram triggered cardiac cine acquisitions were performed in all patients. The maximum gradient performance was 40 mT/m with a slew rate of 200 mT/m/ms. A cardiac phased-array coil was used for signal reception. An axially acquired stack covering the whole heart (18–24 slices, no gap) as well as a short-axis stack covering the entire left and right ventricles (12–16 slices, no gap) was utilized with cine steady-state free-precession acquisitions (TR/TE/flip angle = 2.7 ms/1.35 ms/42°) for the assessment of heart function in all four cardiac chambers and morphology. Global, basal, midventricular and apical right ventricular strain and strain rate was quantified by applying cine 4-chamber long axis and cine short axis views. Longitudinal, circumferential and radial strain and strain rate were assessed. Within one cardiac cycle $>$ 25 heart frames were acquired. At a typical heart rate of 70 beats per minute, the temporal resolution was 34 ms per cardiac frame. Spatial resolution was $1.5 \times 1.5 \times 8$ mm^3.

2.3. Strain analysis

The longitudinal and short axis views served as the quantitative parameter for right ventricular strain assessment. Strain analysis was conducted using the CVI42® software package (Circle Cardiovascular Imaging Inc., Calgary, Canada, Release 5.12.1) based on cine steady-state free-precession acquisitions. Contours of right ventricular endocardium were delineated manually in 4-chamber long-axis slices illustrated by Fig. 1. Global and regional longitudinal, circumferential and radial strain as well as global peak systolic and diastolic strain rate were quantified. Regional deformation assessment was attained by division into basal, midventricular and apical strain. Comparisons were made between CA, HCM and CTRL subjects. CA-Subtypes of AL and ATTR were compared. Corresponding volumetric quantifications of the right ventricle were obtained at the end of diastole and systole respectively by defining the endocardial contours in the acquired short axis cine stack.

2.4. Statistics

Statistical analysis was performed using SPSS (version 27.0.0.0, IBM Deutschland GmbH). Continuous variables were presented as mean ± standard deviation (SD) when normally distributed, otherwise as median with interquartile range. Comparison of baseline characteristics, volumetric parameters and cardiac strain between three different groups were carried out using univariate ANOVA if criteria were met. In the case of homogeneity of variance, post hoc Tukey-HSD was performed; otherwise, ANOVA-Welch and post-hoc Games-Howell analysis was used to detect differences between groups. In the absence of a normal distribution and extreme outliers, the Kruskal-Wallis test was used instead. Comparison between amyloidosis subtypes was carried out using unpaired Student’s *t*-test for parametric data sets or the Mann-Whitney-*U* test for a non-parametric data-set. P-values of < 0.05 were considered statistically significant. Global strain differences were presented as box plot graphs (Fig. 2). Regional circumferential, longitudinal and radial strains were exhibited in Fig. 3A-C. Additionally, sensitivity and specificity of strain and strain rate between CA- and HCM- patients were analyzed utilizing the receiver operating characteristic (ROC)-analysis, demonstrated in Fig. 4. The area under the curve (AUC) ranges were defined for 0.9–0.99 as an excellent test, 0.8 – 0.89 as a good test, 0.7–0.79 as a fair test and < 0.7 as a non-useful test [19]. Complementary, the optimal sensitivity and specificity was given by the Youden-Index. A binomial logistic regression was performed to determine the effect of age, heart rate, right ventricular ejection fraction (RV-EF), left ventricular ejection fraction (LV-EF) and right ventricular global radial strain (GRS) to predict the likelihood to distinguish CA from HCM.

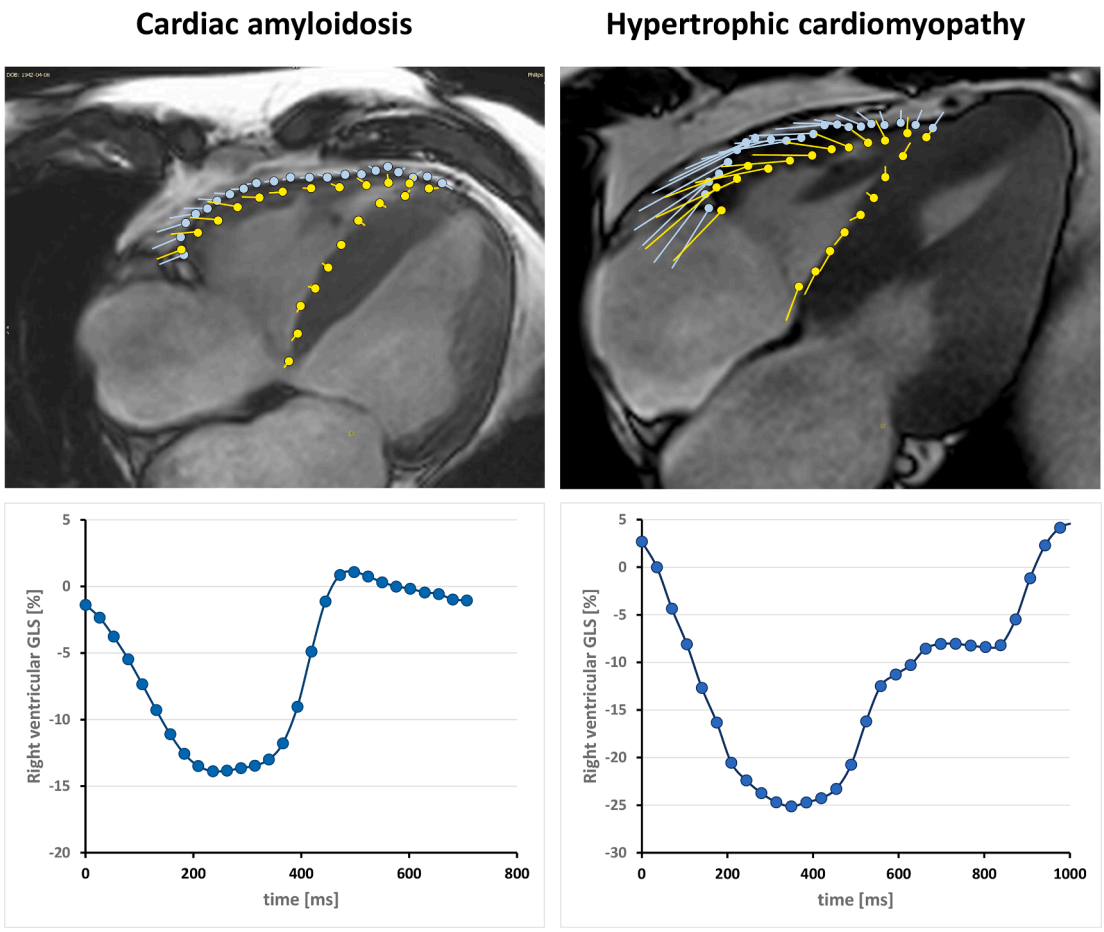

Fig. 1. Feature tracking of the endocardial and epicardial right ventricle in four chamber view of a CA- and HCM- patient with corresponding global longitudinal strain curves.

3. Results

3.1. Baseline characteristics of patients and healthy control subjects

This study included 47 CTRL subjects, 43 CA patients and 20 HCM patients. The median patient age (interquartile range) of CA patients was 79 (14) years, significantly older compared to HCM patients and CTRL subjects. Median BMI was lowest for CA patients with 24.6 (3.9) kg/m^2. Functional cardiac parameters showed significantly elevated heart rate for CA compared to CTRL subjects and HCM patients. Right ventricular indexed end-diastolic volume was significantly greater for CA patients with 87.6 ± 20.2 ml/m^2 compared to HCM-patients and CTRL subjects (all $p < 0.02$). The RV-EF was significantly impaired ($p < 0.001$) and lowest for CA patients with 36.4 ± 13.4 % compared to HCM and CTRL. Details on baseline characteristics of all groups are summarized in Table 1.

3.2. Right ventricular strain and strain rate

Significant CA differentiation from HCM and CTRL subjects was achievable with GLS (global longitudinal strain), GRS (global radial strain) and GCS (global circumferential strain), with greatest significant discrimination for GRS ($p < 0.001$). Global strains are exhibited in Fig. 2. CA patients presented significantly reduced global radial strain (11.7 (5.3) %) and global circumferential strain (7.6 (4.0) %) compared to all other groups (all $p < 0.02$). Regarding strain rates, CA differentiation from HCM was only observed for radial peak systolic strain rate ($p = 0.001$). Both systolic and diastolic radial and circumferential strain rates could discriminate between CA patients and CTRL subjects (all $p \leq 0.002$). HCM differentiation from CA patients was mostly found inconsistent for strain rate data.

Statistically significant CA differentiation from HCM and CTRL subjects was additionally found for left ventricular global strain parameters ($P < 0.001$). Further details on ventricular strain and strain rate are presented in Table 2.

3.3. Regional right ventricular strain

Basal, mid and apical longitudinal strain (LS) showed no significant difference between CA patients and CTRL subjects. However, CA discrimination from HCM patients was achievable for all regional LS ($p \leq 0.007$). Moreover, basal and midventricular radial strain (RS) exhibited significant CA differentiation from HCM (all ≤ 0.006) and CTRL (all $p < 0.001$). Circumferential strain (CS) only differentiated CA from HCM at midventricular level ($p < 0.05$). No CA discrimination from HCM was observable at apical level for both radial and circumferential strain. Regional strain differences are summarized in Table S1 and illustrated in Fig. 3A-C.

3.4. ATTR vs AL subtypes

The heart rate of CA patients with AL subtype (78 ± 12 bpm) was significantly higher ($p = 0.01$) in contrast to the ATTR subtype (68 ± 12 bpm). Otherwise, volumetric, global and regional strain features showed no significant difference between both CA subtypes, as exhibited by Table 3.

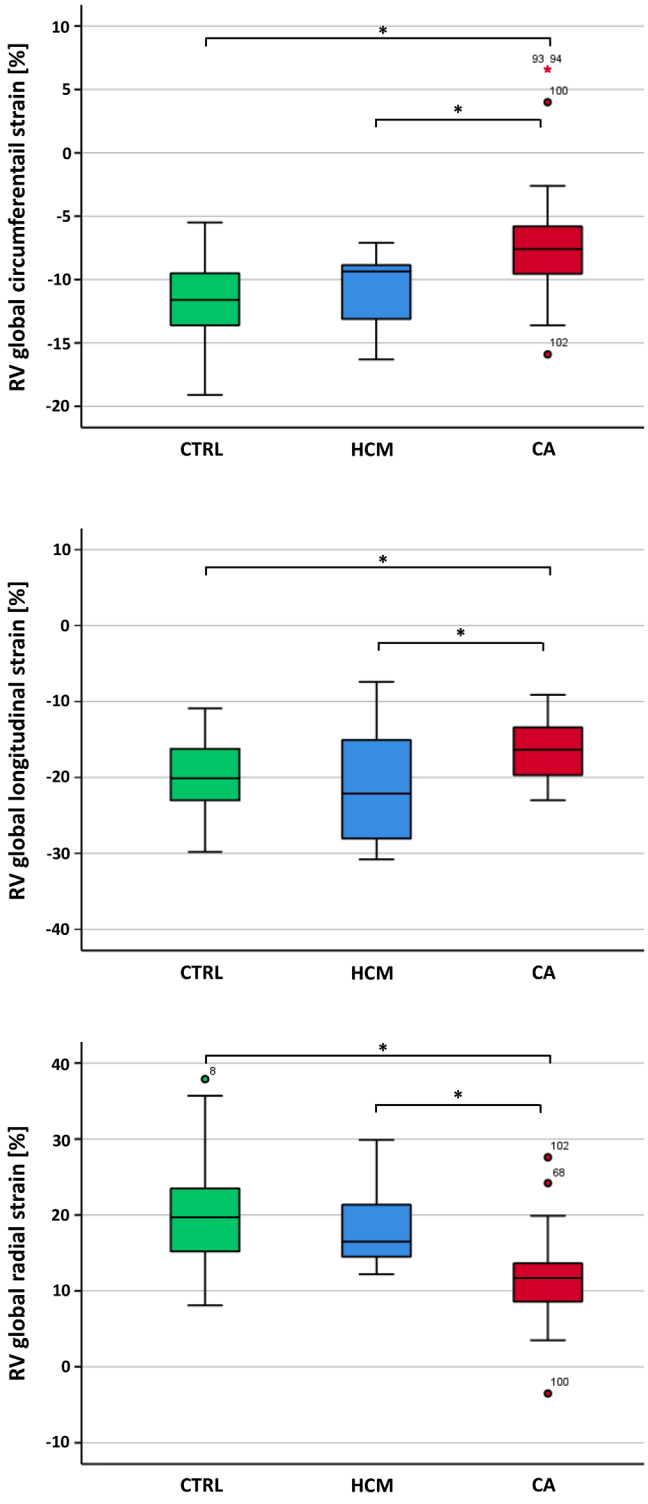

Fig. 2. Box plots of the right ventricular global circumferential, longitudinal and radial strain of CTRL subjects, HCM- and CA-patients. *statistical significance.

3.5. Sensitivity and specificity of right ventricular strain and strain rate for HCM and CA patients

ROC analyses found longitudinal and circumferential strain as a "fair" diagnostic test (AUC = 0.740, 0.758) for CA differentiation from HCM. Global radial strain and systolic radial strain rate were identified as "good" diagnostic tests (AUC = 0.859, sensitivity = 100 %, specificity = 60.5 % resp. AUC = 0.820, sensitivity = 75 %, specificity = 72.1 %). The remaining strain rates categorized as "non-useful" (AUC < 0.700). Cut-off and AUC values are summarized in Table 4 and illustrated in Fig. 4.

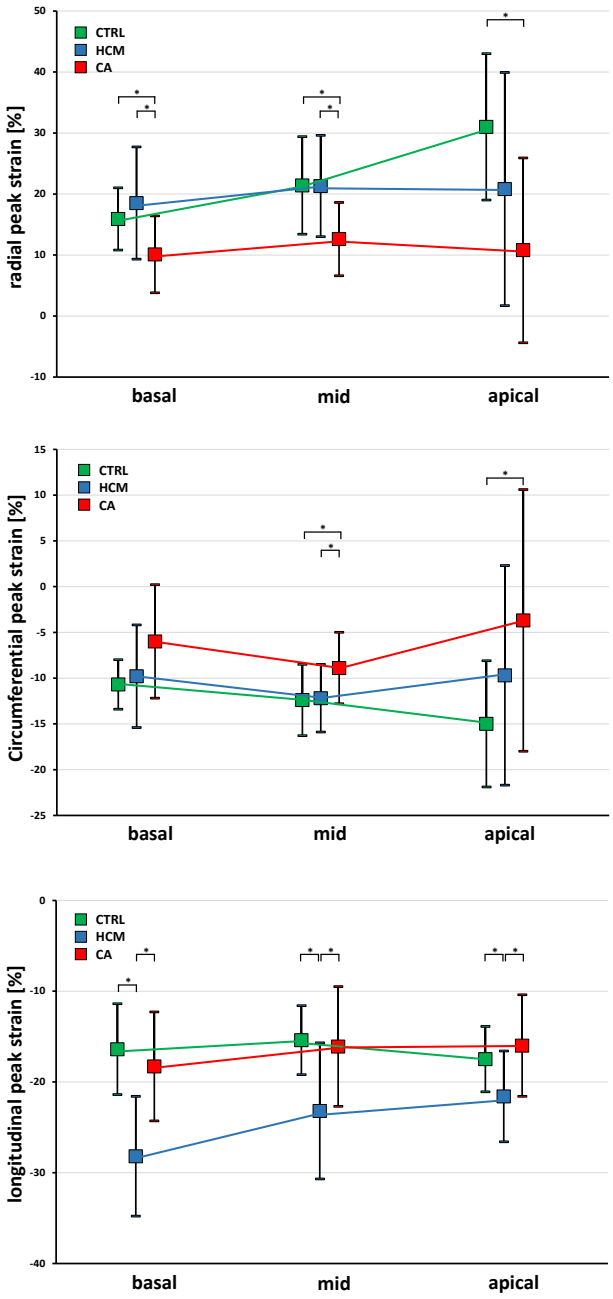

Fig. 3. Regional right ventricular a) radial, b) circumferential and c) longitudinal strain at basal, mid and apical level for control subjects, HCM- and CA-patients. Values are presented as mean ± standard deviation. * statistically significant different.

3.6. Binominal logistic regression model

The binomial logistic regression model was statistically significant, $\chi^2(5) = 51.761$, $p < 0.001$, resulting in a large amount of explained variance [20], as shown by Nagelkerke's R2 = 0.791. Overall percentage of accuracy in classification was 91.9%, with a sensitivity of 95.2% and a specificity of 85.0%. Goodness-of-fit was assessed using the Hosmer-Lemeshow-Test, indicating a good model fit, $\chi^2(8) = 9.636$, $p > 0.05$.

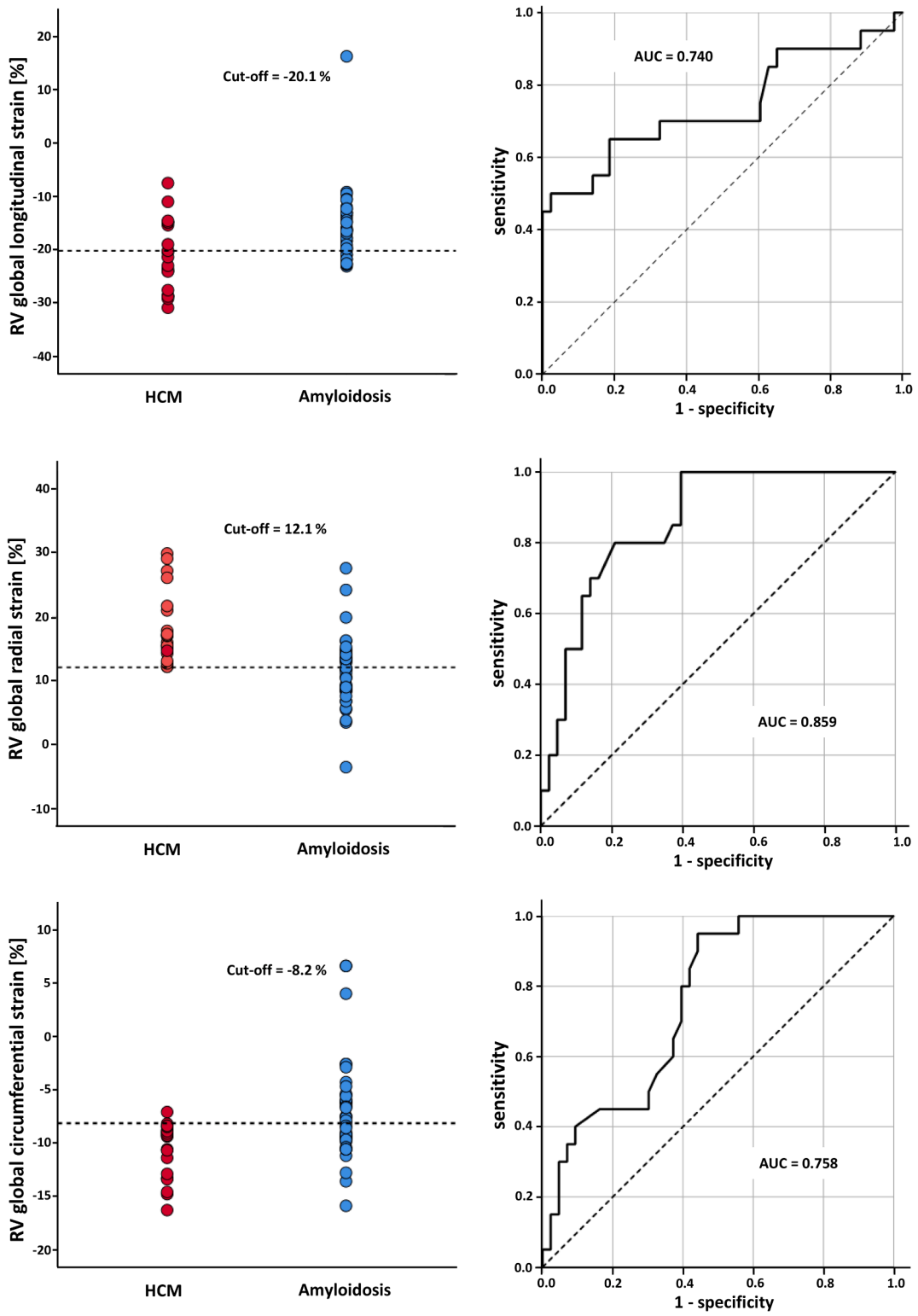

Fig. 4. ROC Analysis of right ventricular global longitudinal, radial and circumferential strain between HCM- and CA patients.

Of the five variables entered into the regression model, two contributed significantly in predicting CA: heart rate ($p = 0.046$) and RV-EF ($p = 0.017$), while the other variables showed no significant effect: age ($p = 0.059$), LV-EF ($p = 0.531$) nor RV-GRS ($p = 0.617$). HCM patients were coded as "0″ and CA patients as "1" in the binominal logistic regression model, which means that odds ratios > 1 indicate a higher probability of the presence of "CA", whereas odds ratios < 1 indicate a lower probability of the presence of "CA". According to this definition, the lower RV-EF (OR = 0.833, 95%-CI [0.716, 0.968]) or the higher heart rate (OR = 1.133, 95%-CI [1.002, 1.280]) found in this study are in support of amyloidotic cardiomyopathy. All model coefficients and odds can be found in Table 5.

Table 1
Baseline parameters and right ventricular function of patients with cardiac amyloidosis and hypertrophic cardiomyopathy. Comparison to healthy control subjects. Depending on the prerequisites, either ANOVA or the Kruskal-Wallis test was applied as global tests to detect differences between the three groups. In case of significance, the appropriate post-hoc tests were used to identify statistically significant differences between pairs.

	CTRL	HCM	CA	Comparison	Post-Hoc Test
N	47	20	43		
Sex [males]	25	10	32		
Age [yrs] [b]	55.9 (10.4)[a]	63.9 ± 7.4	79 (14)[a]	CTRL-CA HCM-CA CTRL-HCM	p < 0.001 p < 0.001 p = 0.007
Weight [kg] [c]	74.8 ± 12.8	83.6 ± 12.8	76.3 ± 14.8	–	n.s.
Height [cm] [c]	172.7 ± 10.7	171.7 ± 9.2	173.4 ± 10.3	–	n.s.
BSA [m^2] [c]	1.88 ± 0.21	1.96 ± 0.18	1.89 ± 0.22	–	n.s.
BMI [kg/m^2] [d]	25.0 ± 2.7	28.3 ± 3.9	24.6 (3.9)[a]	CA-HCM CTRL-HCM	all p < 0.001
HR [bpm] [d]	64.9 ± 9.7	63.1 ± 7.8	74.0 ± 14.8	HCM-CA CTRL-CA	all p < 0.001
RV-EDV_i [ml/m^2] [b]	76.4 ± 12.7	70.4 ± 11.9	87.6 ± 20.2	CTRL-CA HCM-CA	p = 0.014 p < 0.001
RV-ESV_i [ml/m^2] [b]	30.4 ± 8.2	30.9 ± 10.4	55.4 ± 18.1	CTRL-CA HCM-CA	all p < 0.001
RV-SV_i [ml/m^2] [d]	46.1 ± 6.8	39.5 ± 11.7	32.0 (25.0)[a]	CA-CTRL HCM-CTRL	p < 0.001 p = 0.023
RV-EF [%] [b]	60.7 ± 5.7	65.0 (13.0)[a]	36.4 ± 13.4	CTRL-CA HCM-CA	all p < 0.001
LV-EDV_i [ml/m^2] [d]	72.4 ± 10.1	74.0 (13.8)[a]	68.8 (22.0)[a]	CA-CTRL	P = 0.049
LV-ESV_i [ml/m^2] [d]	23.2 (7.2)[a]	22.8 ± 9.6	26.7 (23.7)[a]	–	n.s.
LV-SV_i [ml/m^2] [d]	48.1 ± 6.1	49.4 ± 10.7	36.9 (14.3)[a]	CA-CTRL CA-HCM	all p < 0.001
LV-EF [%] [d]	66.7 ± 5.0	72.2 ± 8.6	60.2 (15.0)[a]	CA-CTRL CA-HCM CRTL-HCM	p < 0.001 p < 0.001 p < 0.029

CTRL – healthy control subjects, HCM – hypertrophic cardiomyopathy patients, CA – cardiac amyloidosis patients, BSA – body surface area, BMI – body mass index, HR – heart rate, EDVi – indexed end-diastolic volume, ESVi – indexed end-systolic volume, SVi – indexed stroke volume, EF - ejection fraction, RV – right ventricular, LV – left ventricular.
[a] – median value (interquartile range).
[b] - ANOVA-Welch.
[c] – ANOVA-Tukey-HSD.
[d] - Kruskal -Wallis –Test.

Table 2
Right ventricular strain and strain rates of patients with cardiac amyloidosis and hypertrophic cardiomyopathy. Comparison to healthy control subjects. Depending on the prerequisites, either ANOVA or the Kruskal-Wallis test was applied as global tests to detect differences between the three groups. In case of significance, the appropriate post-hoc tests were used to identify statistically significant differences between pairs.

	CTRL	HCM	CA	Comparison	Post-Hoc Test
RV strain					
GLS (4-chamber) [%] [b]	−19.8 ± 4.8	−21.3 ± 6.7	−16.5 ± 3.9	CA-HCM CA-CTRL	p = 0.032 p = 0.004
GRS (short axis) [%] [d]	19.7 (8.5)[a]	16.5 (7.1)[a]	11.7 (5.3)[a]	CA-HCM CA-CTRL	p < 0.001 p < 0.001
GCS (short axis) [%] [d]	−11.7 ± 3.0	−9.4 (4.4)[a]	−7.6 (4.0)[a]	CA-HCM CA-CTRL	p = 0.015 p < 0.001
RV strain rate					
GLSR-syst [s^{-1}] [d]	−1.1 (0.5)[a]	−1.2 (0.5)[a]	−1.2 (0.7)[a]	–	n.s.
GLSR-dias [s^{-1}] [d]	1.2 (0.6)[a]	1.05 (0.55)[a]	1.1 (0.5)[a]	–	n.s.
GRSR-syst [s^{-1}] [d]	0.9 (0.5)[a]	0.96 ± 0.24	0.6 (0.4)[a]	CA-CTRL CA-HCM	p < 0.001 p = 0.001
GRSR-dia [s^{-1}] [d]	−1.0 (0.5)[a]	−0.7 (0.4)[a]	−0.5 (0.4)[a]	CA-CTR HCM-CRTL	p < 0.001 p = 0.037
GCSR-syst [s^{-1}] [d]	−0.6 (0.3)[a]	−0.65 (0.2)[a]	−0.4 (0.3)[a]	CA-CTRL	p = 0.002
GCSR-dia [s^{-1}] [b]	0.64 ± 0.16	0.48 ± 0.12	0.44 ± 0.18	CA-CTRL HCM-CRTL	p < 0.001 p < 0.001
LV strain					
LV-GLS [%] [c]	−17.3 ± 1.7	−11.2 ± 2.4	−8.5 ± 2.6	CA-HCM CA-CTRL HCM-CTRL	all p < 0.001
LV-GRS [%] [c]	36.5 ± 7.3	26.7 ± 7.1	16.8 ± 5.4	CA-HCM CA-CTRL HCM-CTRL	all p < 0.001
LV-GCS [%] [c]	−19.9 ± 2.4	−15.5 ± 2.8	−11.6 ± 2.9	CA-HCM CA-CTRL HCM-CTRL	all p < 0.001

n.s. – not significant, CA – cardiac amyloidosis patients, CTRL – healthy control subjects, HCM – hypertrophic cardiomyopathy patients, RV – right ventricular, GLS – global longitudinal strain, GRS – global radial strain, GCS – global circumferential strain, syst. – peak systolic, dia – peak diastolic, GLSR – global longitudinal strain rate, GRSR – global radial strain rate, GCSR – global circumferential strain rate, LV-GLS – left ventricular global longitudinal strain, LV-GCS – left ventricular global circumferential strain, LV-GRS – left ventricular global radial strain.
[a] – median value (interquartile range).
[b] - ANOVA-Welch.
[c] - ANOVA-Tukey-HSD.
[d] - Kruskal -Wallis –Test.

3.7. Association between RV global strain and cardiac function and baseline parameters

The univariate correlation analysis of RV global strain and cardiac function and baseline parameters in CA patients showed statistically significant ($P < 0.05$) moderate correlations for RV-GRS with RV-EF (Spearman's $= 0.584$), RV-EDV_i ($\rho = -0.301$), RV-ESV_i ($\rho = -0.479$), and LV-EF ($\rho = 0.539$). Moderate correlations were also found for RV-GCS with RV-EF ($\rho = -0.503$), RV-EDV_i ($\rho = 0.314$), RV-ESV_i ($\rho = 0.443$), and LV-EF ($\rho = -0.440$). RV-GLS only correlated with RV-ESV_i ($\rho = 0.331$). For global RV strain, there were no correlations with RV-SV_i, age, and heart rate.

Multiple linear regression analysis was conducted to examine the associations of RV global strain with RV-EF, LV-EF, age and heart rate. RV-EDV_i, RV-ESV_i and RV-SV_i were not included in the analysis because

Table 3
Differentiation between ATTR and AL subtypes of cardiac amyloidosis patients.

	ATTR	AL	p-value
N	**21**	**20**	
right ventricular volumes			
EDV_i [ml/m²] [b]	87.5 ± 21.1	87.7 ± 19.8	p = 0.985
ESV_i [ml/m²] [b]	55.3 ± 17.9	55.5 ± 18.6	p = 0.978
SV_i [ml/m²] [b]	32.2 ± 12.9	32.2 ± 12.6	p = 0.993
EF [%] [b]	36.3 ± 13.2	36.4 ± 13.9	p = 0.988
HR [bpm] [b]	68 ± 12	78 ± 12	p = 0.010
right ventricular strain			
GLS (4-chamber) [%] [b]	−17.2 ± 4.1	−15.8 ± 3.6	p = 0.245
GRS (short axis) [%] [c]	10.3 ± 5.6	12.0 (5.7)[a]	p = 0.106
GCS (short axis) [%] [c]	−6.2 (4.0)[a]	−8.4 (3.9)[a]	p = 0.103
Regional right ventricular longitudinal strain			
Basal (4-chamber) [%] [b]	−18.2 ± 5.2	−18.5 ± 7.1	p = 0.908
Mid (4-chamber) [%] [c]	−17.9 ± 5.9	−13.9 ± 6.8	p = 0.083
Apical (4-chamber) [%] [c]	−16.1 ± 6.2	−15.8 ± 4.9	p = 0.876
Apical sparing [ ]	0.46 ± 0.18	0.52 ± 0.17	p = 0.381

ATTR – transthyretin related amyloidosis, AL – light chain amyloidosis, EDV_i – indexed right ventricular end-diastolic volume, ESV_i – indexed right ventricular end-systolic volume, SV_i – indexed right ventricular stroke volume, EF - right ventricular ejection fraction, HR – heart rate, GLS – global longitudinal strain, GRS - global radial strain, GCS - global circumferential strain.
[a] – median value (interquartile range).
[b] – Unpaired *t*-test.
[c] – Mann-Whitney *U* Test.

Table 4
ROC analyses of right ventricular strain and strain rate for differentiation of patients suffering cardiac amyloidosis and hypertrophic cardiomyopathy, respectively.

	Cut-off value	AUC	Sensitivity [%]	Specificity [%]	Quality
right ventricular strain					
GLS [%]	−20.1	0.740*	65.0	81.4	fair
GRS [%]	12.1	0.859*	100	60.5	good
GCS [%]	−8.15	0.758*	95.0	55.8	fair
right ventricular strain rate					
GLSR-syst. [s^{-1}]	–	0.502	–	–	non-useful
GLSR-dia. [s^{-1}]	–	0.531	–	–	non-useful
GRSR-syst. [s^{-1}]	0.75	0.820*	75.0	72.1	good
GRSR-dia. [s^{-1}]	–	0.649	–	–	non-useful
GCSR-syst. [s^{-1}]	−0.45	0.697*	90.0	51.2	non-useful
GCSR-dia. [s^{-1}]	–	0.578	–	–	non-useful

AUC – area under curve, CA – cardiac amyloidosis patients, HCM – hypertrophic cardiomyopathy patients, GLS – global longitudinal strain, GRS - global radial strain, GCS - global circumferential strain.
* Statistically significant.

of multicollinearity with RV-EF. Statistically significant associations were found between RV-GRS and RV-EF ($\beta = 0.520$, $P = 0.001$) and RV-GCS and RV-EF ($\beta = -0.479$, $P = 0.002$), respectively (Table 6).

4. Discussion

Morphological differentiation between HCM and CA patients is challenging. Although some studies have demonstrated significant RV strain difference between CA patients and CTRL subjects [1,12,21], CMR data on RV strain for differentiation of the hypertrophic phenotype remains very limited. To date, only one recent CMR study has compared CA and HCM functional phases of RV strain. However, to our best knowledge the CMR study presented here is the first to assess regional differences in RV deformation for comprehensive discrimination of the hypertrophic phenotype and CA subtypes ATTR and AL. This study presents a series of important findings:

1. GLS, GRS and GCS significantly discriminate CA from HCM and CTRL.
2. GRS qualifies as a "good" diagnostic feature for hypertrophic phenotype differentiation.
3. Various basal, mid and apical strain differentiate CA from HCM and CTRL.
4. ATTR and AL subtypes present comparable levels of right ventricular impairment.
5. RV-EF is a valuable and efficient clinical predictor of CA.

4.1. Global RV strain differentiation

The differentiation of CA and HCM patients based on global left ventricular strain is well known and could also be confirmed in our study. However, this study also presents CMR as a clinically valuable method for quantifying RV strain in such patients. The data from our study support the differentiation of CA from CTRL subjects and HCM patients, based on right ventricular GRS, GCS and GLS, consistent with previous literature [11,12]. In contrast to functional parameters of the left ventricle [5], specific functional parameters such as right ventricular ejection fraction provide additional discriminative power between CA and HCM patients as substantiated by our logistic regression analysis. Furthermore, multiple linear regression analysis found RV-EF to be the dominant factor explaining the association with impaired global RV strain. Notably, impairment of ejection fractions appears more severe in the right rather than the left ventricle, characterizing RV-EF as a valuable predictor that is routinely available.

Consistent with global strain rate data from Liu and colleagues[11], we observed no statistical difference for diastolic and systolic longitudinal strain rate. Despite significant difference in systolic radial strain rate between CA and HCM, strain rate data otherwise appear poorly suited for CA-HCM differentiation. This observation is substantiated by recent CMR data, whereby sporadic significant differences in strain rate data exhibit no promising clinical utility [11].

4.2. Regional RV strain differentiation

In contrast to the regional LS of the left ventricle [21], regional LS of the RV appears more comparable between CA patients and CTRL subjects. Comparable regional LS between CA and CTRL may be the result of delayed impairment of RV diastolic function, as RV involvement has been shown to occur later than that of the LV [1]. In the present study, more pronounced differences in right ventricular LS were observed between CA and HCM patients, which is consistent with previous echocardiographic findings [9]. Arvidsson and colleagues underscored the echocardiographic challenge of visualizing the RV free wall, complicated by its movement out of the field of view. This may explain why only basal and apical free wall strain significantly differed between CA

Table 5
Binominal logistic regression to predict the likelihood to distinguish CA from HCM.

	Regression coefficient B	Standard error	Wald	p	Odds ratio	95 % CI for Odds ratio	
						Lower bound	Upper bound
age	0.115	0.061	3.559	0.059	1.122	0.996	1.264
Heart rate	0.125	0.062	3.993	0.046	1.133	1.002	1.280
RV-EF	−0.183	0.077	5.650	0.017	0.833	0.716	0.968
LV-EF	0.045	0.072	0.393	0.531	1.046	0.908	1.206
GRS	0.051	0.103	0.251	0.617	1.053	0.861	1.288
constant	−10.278	9.353	1.207	0.272	0.000		

CA – cardiac amyloidosis patients, HCM – hypertrophic cardiomyopathy patients, GRS - global radial strain, RV-EF – right ventricular ejection fraction, LV-EF – left ventricular ejection fraction.

Table 6
Multiple linear regression of right ventricular global strain and cardiac function and baseline parameters in patients with cardiac amyloidosis.

	RV-GRS		RV-GCS		RV-GLS	
	β	P-value	β	P-value	β	P-value
age	−0.042	0.740	0.114	0.368	−0.211	0.173
Heart rate	−0.125	0.331	0.153	0.232	−0.165	0.287
RV-EF	0.520	**0.001**	−0.479	**0.002**	−0.211	0.231
LV-EF	0.238	0.110	−0.270	0.072	−0.282	0.114

β - Standardized regression coefficient, GRS - global radial strain, GCS - global circumferential strain, GLS - global longitudinal strain, RV-EF – right ventricular ejection fraction, LV-EF – left ventricular ejection fraction.

and HCM patients [9], whereas our study observed differences for all regions of LS. The right ventricular LS data presented here discriminates CA from HCM patients at basal, mid and apical level, emphasizing its clinical value for hypertrophic phenotype differentiation. Moreover, basal and mid RS differentiated CA from both HCM and CTRL. Basal and mid RS exhibit significant RV wall impairment of CA patients, characterizing the restrictive nature of the amyloidotic cardiomyopathy. Complemented by its "good" diagnostic sensitivity and specificity, RS appears to possess valuable clinical utility for achieving greater accuracy in non-invasive CA diagnostics. Previous comparable echocardiographic data only presented significant strain difference on basal level [21]. It must be noted that their sample size was limited to five CA patients and five CTRL subjects. To the best of our knowledge no other CMR data to date is available for analytic comparison. However, overall the significances for regional strain differences present in a non-uniform pattern, challenging implementation into routine clinical practice.

4.3. Subtype differentiation between AL and ATTR

Consistent with left ventricular strain data [2], our study found similar degrees of impairment in global and regional RV strain between CA subtypes AL and ATTR. Previous differentiation in CA subtypes was primarily based on electrocardiographic, echocardiographic, hemodynamic data [22] and alterations in late gadolinium enhancement patterns [3]. The more rapid disease progression of the AL-subtype has been postulated to be associated with differences in frequency of amyloid deposition. ATTR patients presumably undergo a slower deposition of transthyretin related fibrils, enabling development of regional cardiac compensatory mechanisms, characterized by a more stable clinical progression. Differences in global and regional deformation of the right ventricular myocardium do not reflect differences in deposition frequency and thus provide no basis for subtype differentiation.

4.4. Future implications of RV strain

The prognosis and therapeutic strategies greatly differ between CA and HCM patients, emphasizing the need for an improved diagnostic approach of hypertrophic phenotype differentiation. Furthermore, common renal insufficiency among amyloidotic patients demands diagnostic non-contrast alternatives. Implementation of reliable strain profiles in clinical practice may enhance our ability to discriminate CA patients from other differential diagnosis, facilitating early start of therapy and improving patient prognosis. The complex pattern of strain significances presented by our plethora of data, suggests effective strain differences exist for CA differentiation from CA and CTRL. In times of increased automated contouring and artificial intelligence, future multiparametric algorithms may translate these parameter clusters into more efficient non-contrast, clinical support.

4.5. Limitation

This is a retrospective single-center study with typical limitations. It must be noted that RV strain parameters may have no additional utility beyond left ventricular tissue characterization as native T1 or late gadolinium enhancement findings were not assessed throughout this study due to retrospective data inconsistencies. Additionally, the included cohort remained heterogenous in the aspects electrocardiographic data, nor where patients or subjects' sex-matched. We attempted to provide greater homogeneity by only including healthy subjects above the age of 50 years. Furthermore, overlapping structural changes of hypertensive heart disease cannot be excluded. CA patients were diagnosed in phenotypic stages of disease, no early diagnostic features can be drawn from this study. Nevertheless, this is the first MRI based study to present a profound assessment of right ventricular regional strain of biopsy validated CA patients.

5. Conclusion

All global RV strains and various regional strains possess effective discriminatory value for CA-HCM differentiation. However, in terms of feasible clinical practice, impaired RV-EF was found an effective and routinely available predictor of CA.

Declaration of Competing Interest

The authors declare that they have no known competing financial interests or personal relationships that could have appeared to influence the work reported in this paper.

Acknowledgements

We acknowledge support by the Open Access Publication Funds of the Ruhr-Universität Bochum.

Appendix A. Supplementary material

Supplementary data to this article can be found online at https://doi.org/10.1016/j.ijcha.2022.101167.

References

[1] F. Cappelli, et al., Right ventricular function in al amyloidosis: characteristics and prognostic implication, Eur. Heart J. Cardiovasc. Imaging 13 (2012) 416–422, https://doi.org/10.1093/ejechocard/jer289.

[2] C.C. Quarta, et al., Left ventricular structure and function in transthyretin-related versus light-chain cardiac amyloidosis, Circulation 129 (2014) 1840–1849, https://doi.org/10.1161/CIRCULATIONAHA.113.006242.

[3] J.N. Dungu, et al., Cmr-based differentiation of al and attr cardiac amyloidosis, J. Am. Coll. Cardiol. Img. 7 (2014) 133–142, https://doi.org/10.1016/j.jcmg.2013.08.015.

[4] K. Nochioka, et al., Left atrial structure and function in cardiac amyloidosis, Eur. Heart J. Cardiovasc. Imaging 18 (2017) 1128–1137, https://doi.org/10.1093/ehjci/jex097.

[5] S. Giusca, et al., Multi-parametric assessment of left ventricular hypertrophy using late gadolinium enhancement, t1 mapping and strain-encoded cardiovascular magnetic resonance, J. Cardiovasc. Magn. Reson. 23 (2021) 92, https://doi.org/10.1186/s12968-021-00775-8.

[6] H. Higashi, et al., Restricted left atrial dilatation can visually differentiate cardiac amyloidosis from hypertrophic cardiomyopathy, ESC Heart Fail 8 (2021) 3198–3205, https://doi.org/10.1002/ehf2.13442.

[7] Z. Tan, et al., Left atrial remodeling and the prognostic value of feature tracking derived left atrial strain in patients with light-chain amyloidosis: a cardiovascular magnetic resonance study, Int. J. Cardiovasc. Imaging (2022), https://doi.org/10.1007/s10554-022-02534-x.

[8] D. Bellavia, et al., Utility of doppler myocardial imaging, cardiac biomarkers, and clonal immunoglobulin genes to assess left ventricular performance and stratify risk following peripheral blood stem cell transplantation in patients with systemic light chain amyloidosis (al), J. Am. Soc. Echocardiogr. 24 (2011) 444–454, https://doi.org/10.1016/j.echo.2011.01.003.

[9] S. Arvidsson, M.Y. Henein, G. Wikstrom, O.B. Suhr, P. Lindqvist, Right ventricular involvement in transthyretin amyloidosis, Amyloid 25 (2018) 160–166, https://doi.org/10.1080/13506129.2018.1493989.

[10] A. Malagoli, et al., Multimodality imaging of the ischemic right ventricle: an overview and proposal of a diagnostic algorithm, Int. J. Cardiovasc. Imaging 37 (2021) 3343–3354, https://doi.org/10.1007/s10554-021-02309-w.

[11] H. Liu, et al., Distinguishing cardiac amyloidosis and hypertrophic cardiomyopathy by thickness and myocardial deformation of the right ventricle, Cardiol. Res. Pract. 2022 (2022) 4364279, https://doi.org/10.1155/2022/4364279.

[12] X. Li, et al., Left and right ventricular myocardial deformation and late gadolinium enhancement: incremental prognostic value in amyloid light-chain amyloidosis, Cardiovasc Diagn Ther 10 (2020) 470–480, https://doi.org/10.21037/cdt-20-181.

[13] M. Fontana, et al., Prognostic value of late gadolinium enhancement cardiovascular magnetic resonance in cardiac amyloidosis, Circulation 132 (2015) 1570–1579, https://doi.org/10.1161/CIRCULATIONAHA.115.016567.

[14] R.Y. Kwong, et al., Characterization of cardiac amyloidosis by atrial late gadolinium enhancement using contrast-enhanced cardiac magnetic resonance imaging and correlation with left atrial conduit and contractile function, Am. J. Cardiol. 116 (2015) 622–629, https://doi.org/10.1016/j.amjcard.2015.05.021.

[15] D. Mohty, et al., Prevalence and prognostic impact of left-sided valve thickening in systemic light-chain amyloidosis, Clin. Res. Cardiol. 106 (2017) 331–340, https://doi.org/10.1007/s00392-016-1058-x.

[16] H. Steen, et al., Left and right ventricular strain using fast strain-encoded cardiovascular magnetic resonance for the diagnostic classification of patients with chronic non-ischemic heart failure due to dilated, hypertrophic cardiomyopathy or cardiac amyloidosis, J. Cardiovasc. Magn. Reson. 23 (2021) 45, https://doi.org/10.1186/s12968-021-00711-w.

[17] P.M. Elliott, et al., 2014 esc guidelines on diagnosis and management of hypertrophic cardiomyopathy: the task force for the diagnosis and management of hypertrophic cardiomyopathy of the european society of cardiology (esc), Eur. Heart J. 35 (2014) 2733–2779, https://doi.org/10.1093/eurheartj/ehu284.

[18] S.R. Ommen, et al., 2020 aha/acc guideline for the diagnosis and treatment of patients with hypertrophic cardiomyopathy: a report of the american college of cardiology/american heart association joint committee on clinical practice guidelines, J. Am. Coll. Cardiol. 76 (2020) e159–e240, https://doi.org/10.1016/j.jacc.2020.08.045.

[19] J.V. Carter, J. Pan, S.N. Rai, S. Galandiuk, Roc-ing along: evaluation and interpretation of receiver operating characteristic curves, Surgery 159 (2016) 1638–1645, https://doi.org/10.1016/j.surg.2015.12.029.

[20] K. Backhaus, B. E., W. Plinke, R. Weiber, Multivariate analysemethoden: Eine anwendungsorientierte einführung, Springer, Berlin, 2006.

[21] A. Reddy, et al., Biventricular strain imaging with cardiac mri in genotyped and histology validated amyloid cardiomyopathy, Cardiogenetics 11 (2021) 98–110, https://doi.org/10.3390/cardiogenetics11030011.

[22] C. Rapezzi, et al., Systemic cardiac amyloidoses: disease profiles and clinical courses of the 3 main types, Circulation 120 (2009) 1203–1212, https://doi.org/10.1161/CIRCULATIONAHA.108.843334.